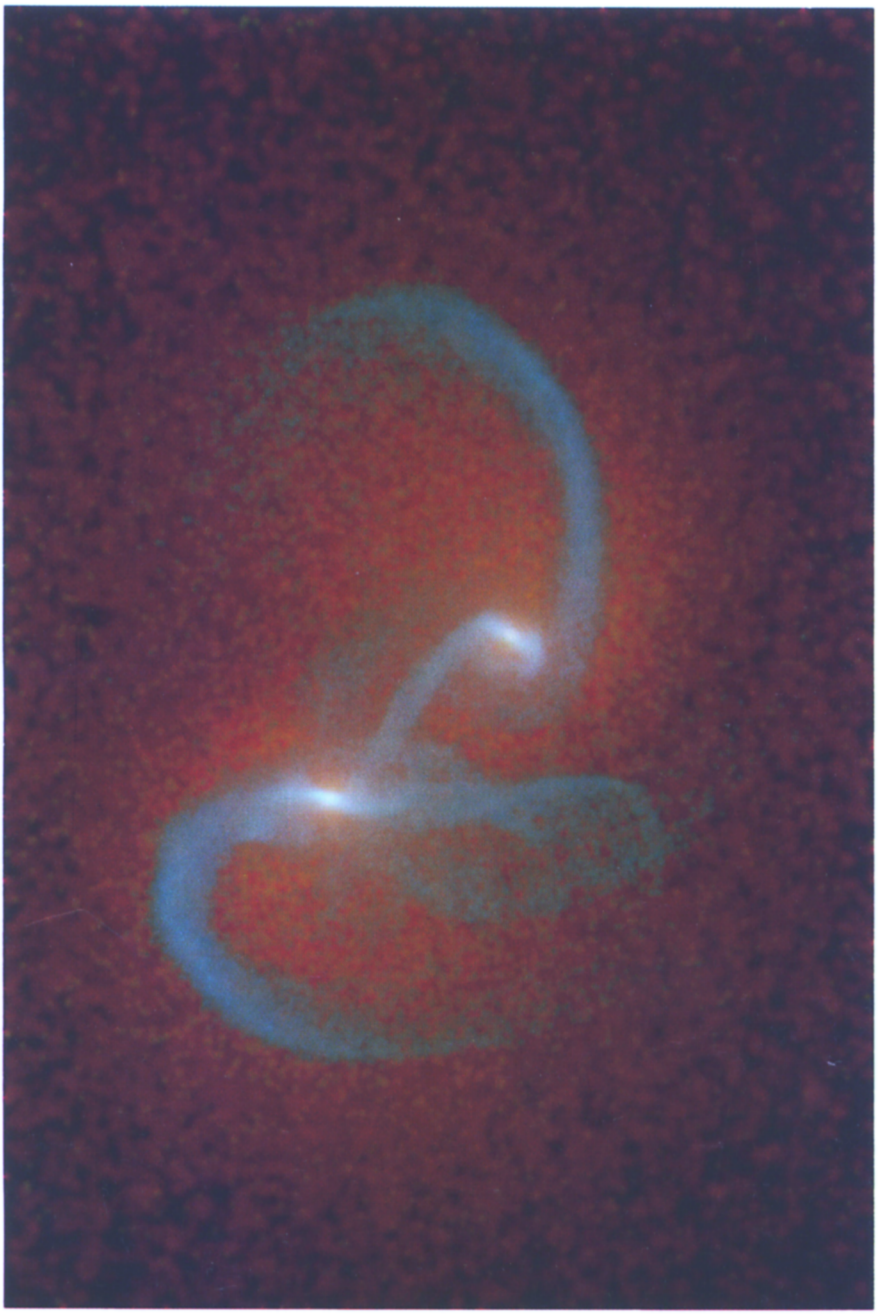

Plate 1. Poster illustration: a parabolic encounter of two disk galaxies, simulated self-consistently with $N = 262144$ particles. In this image, the central bulges are shown in yellow, the disks in blue, and the dark halo material in red.

https://doi.org/10.1017/S0074180900112124 Published online by Cambridge University Press

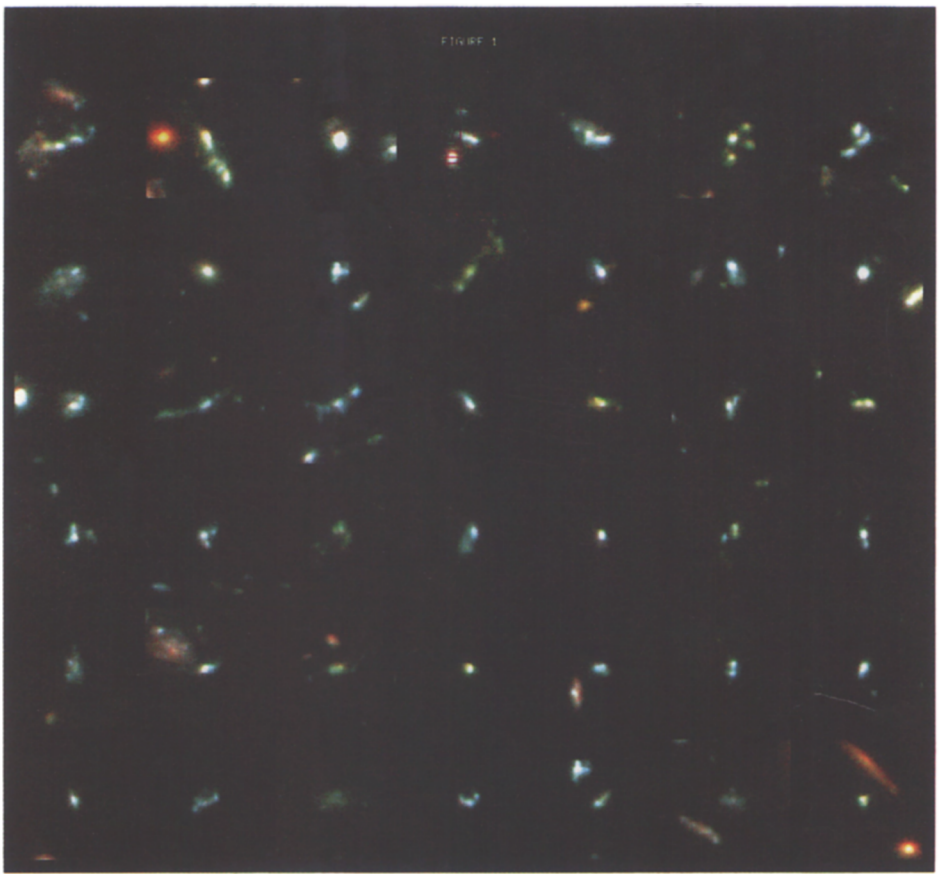

Plate 2. Candidate U_{300}-band dropout Lyman-limit systems in the Hubble Deep Field, with $I < 25$ mag, taken from van den Bergh et al. (1996). "True-color" images were constructed by combining the U_{300},V_{606}, and I_{814}-band observations. [see Abraham, p. 16]

https://doi.org/10.1017/S0074180900112124 Published online by Cambridge University Press

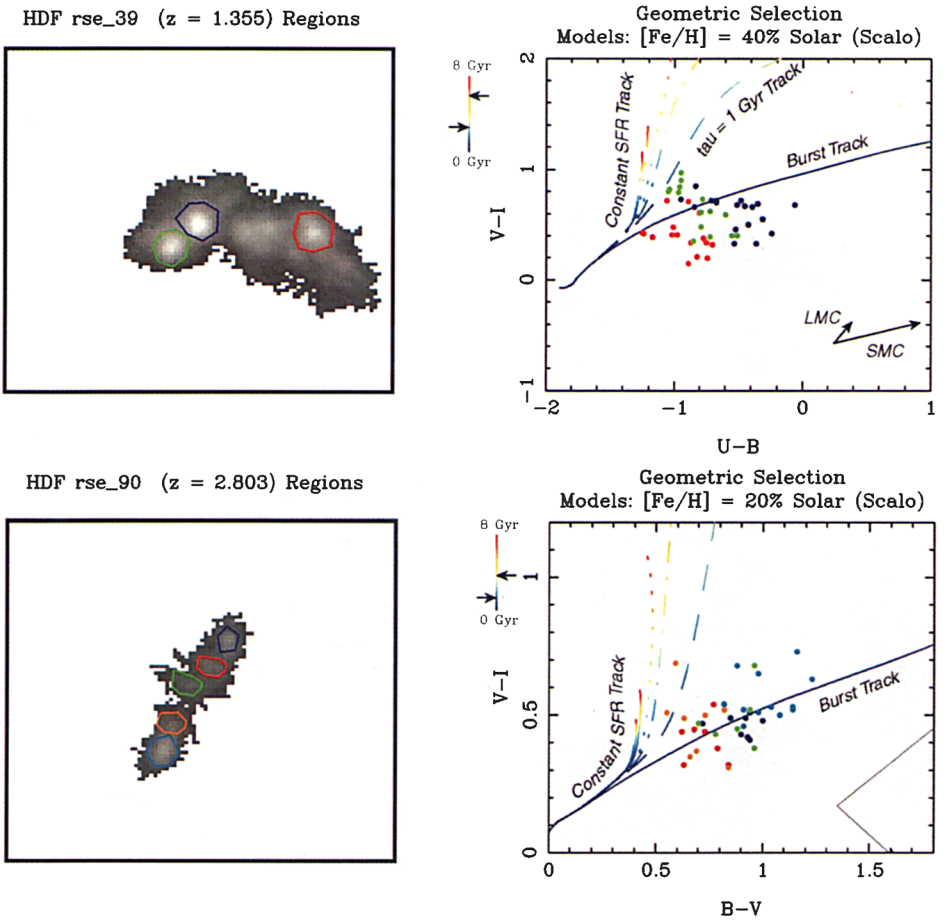

Plate 3. High redshift "chain galaxies" from the HDF (left), and corresponding pixel-by-pixel resolved color-color diagrams (right). Apertures on the images at left enclose subsets of pixels at right. Star-formation history tracks are shown as solid lines, keyed to the colored age bar. Note that both objects are consistent with pure protogalactic starburst tracks with ages < 0.2 Gyr. Synchronization in star-formation activity in the system at $z = 1.355$ (with the ages of bursts changing monotonically with age from a seed knot of star-formation) is seen in many chainlike galaxies. Arrows on the age bar correspond to the age of the universe in an $\Omega = 1$ and a low-Ω Universe. Arrows at the bottom-right corner of the right-hand panels are dust vectors (from Abraham et al., in preparation). [see Abraham, p. 19]

https://doi.org/10.1017/S0074180900112124 Published online by Cambridge University Press

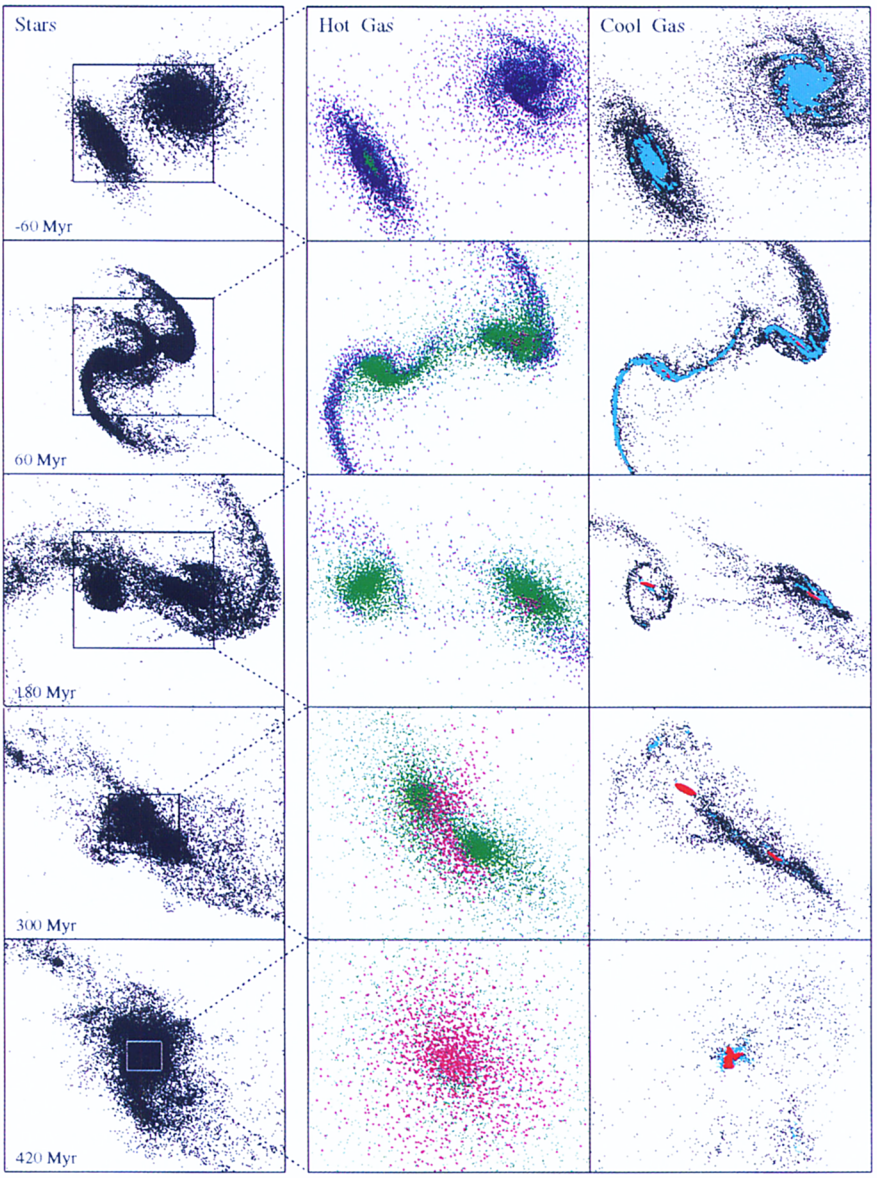

Plate 4. A parabolic encounter of two gas-rich disk galaxies. The stellar distribution is shown on the left; each frame is about 80 × 96 kpc. Times are given with respect to pericenter at $t = 0$. Hot gas is shown in the middle, enlarged with respect to the stellar frame as indicated; color codes temperature, with dark blue, green, and purple indicating factor-of-ten increases up to 2×10^6 K. Cool gas is shown on the right, on the same scale as the hot gas; here color codes local smoothed density, with black, light blue, and red indicating successive factor-of-hundred increases up to $10^2\,\mathrm{cm}^{-3}$. [see Barnes, p. 142]

https://doi.org/10.1017/S0074180900112124 Published online by Cambridge University Press

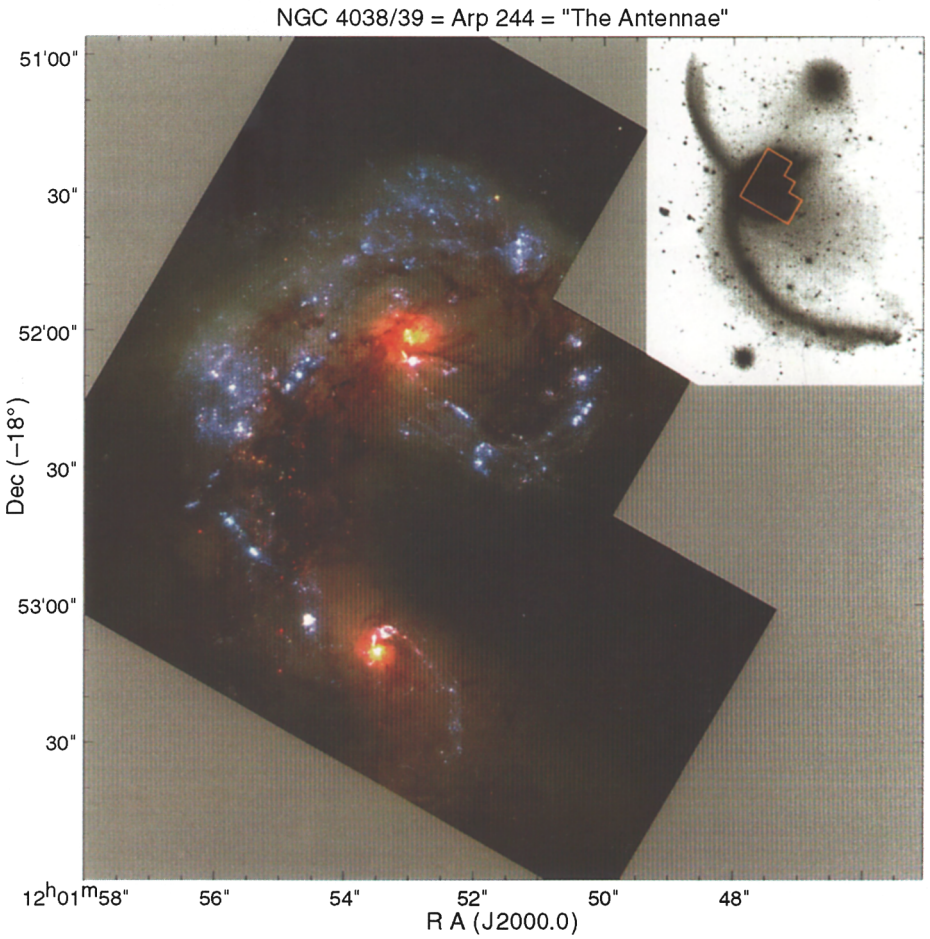

Plate 5. *HST*/WFPC2 image of NGC 4038/39 ("The Antennae") from Whitmore et al. (1998). The insert shows a deep exposure ground-based optical image (courtesy of F. Schweizer) that illustrates the extent of the tidal tails. [see Whitmore, p. 254]

https://doi.org/10.1017/S0074180900112124 Published online by Cambridge University Press

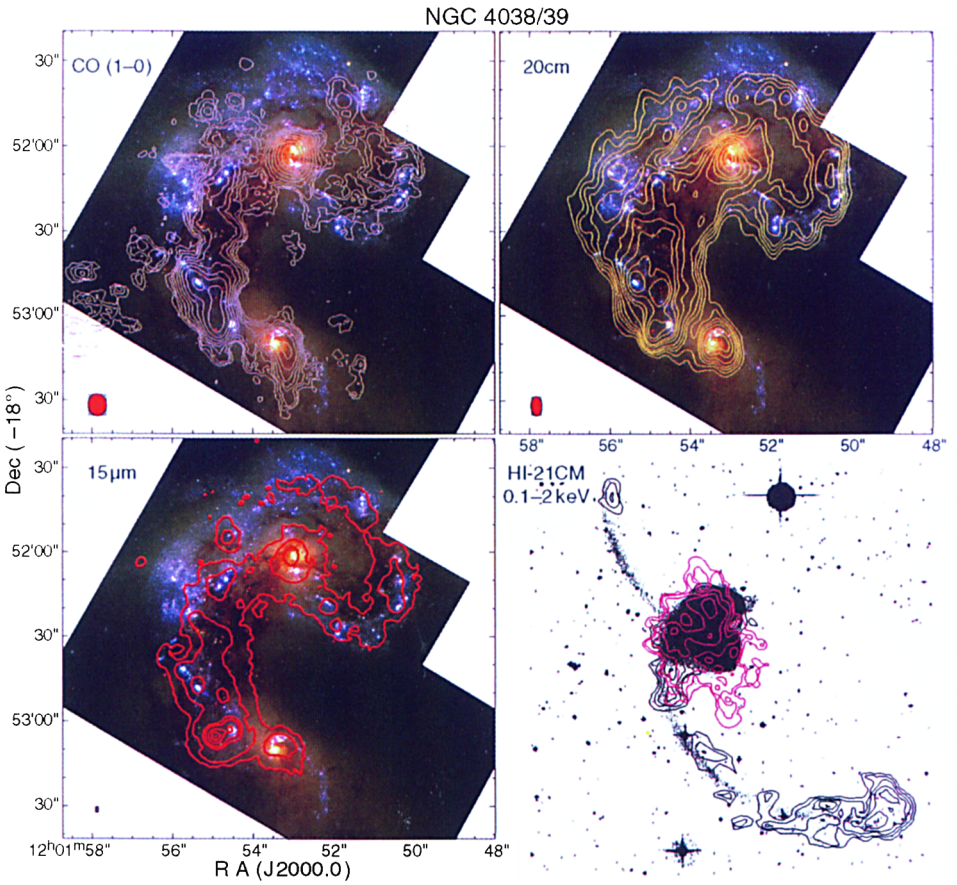

Plate 6. Multiwavelength maps of NGC 4038/39. (upper right) VLA 20 cm radio continuum map. The contour levels are 12,18,24,30,40,60,80,100,150,200 sigma where 1 σ is 0.04 mJy/beam. (upper left) Berkeley-Illinois-Maryland-Array (BIMA) CO(1→0) map. The radio continuum and CO data were kindly provided by Fred Lo, Yu Gao, Siow-Wang Lee, and Robert Gruendl in advance of publication. (lower left) *ISO* 15μm continuum map. The ISOCAM contours are 0.4, 1, 3, 5, 10, and 15 mJy (Mirabel et al. 1998, *A&A*,**333**,L5). (lower right) VLA 21 cm-line data (Hibbard & van Gorkom 1996,*A.J.*,**111**,655), and contours of soft X-Ray emission (0.1–2 KeV) emission detected with *ROSAT* (Read et al. 1995, *MNRAS*,**277**,397). The molecular gas originally in the pre-merger disks of NGC 4038 and NGC 4039 has responded to the merger encounter by producing a large North-South concentration to the East of the two galaxy nuclei, in the "overlap" region from which extend the two long tidal tails. Additional concentrations of molecular gas are found around each nucleus and as part of the "ring" of star formation in the western part of the NGC 4038 disk. The most intense mid-infrared peak produces ~15% of the total 12.5–18 μm emission, and corresponds to an optically obscured knot of ~50 pc radius located in the southern portion of the major concentration of CO emission in the overlap region. This multiwavelength view of NGC 4038/39 illustrates the fact that caution must be applied when trying to interpret galaxy morphology or star-formation rates based on UV-optical data alone. [see Sanders et al. p. 291]

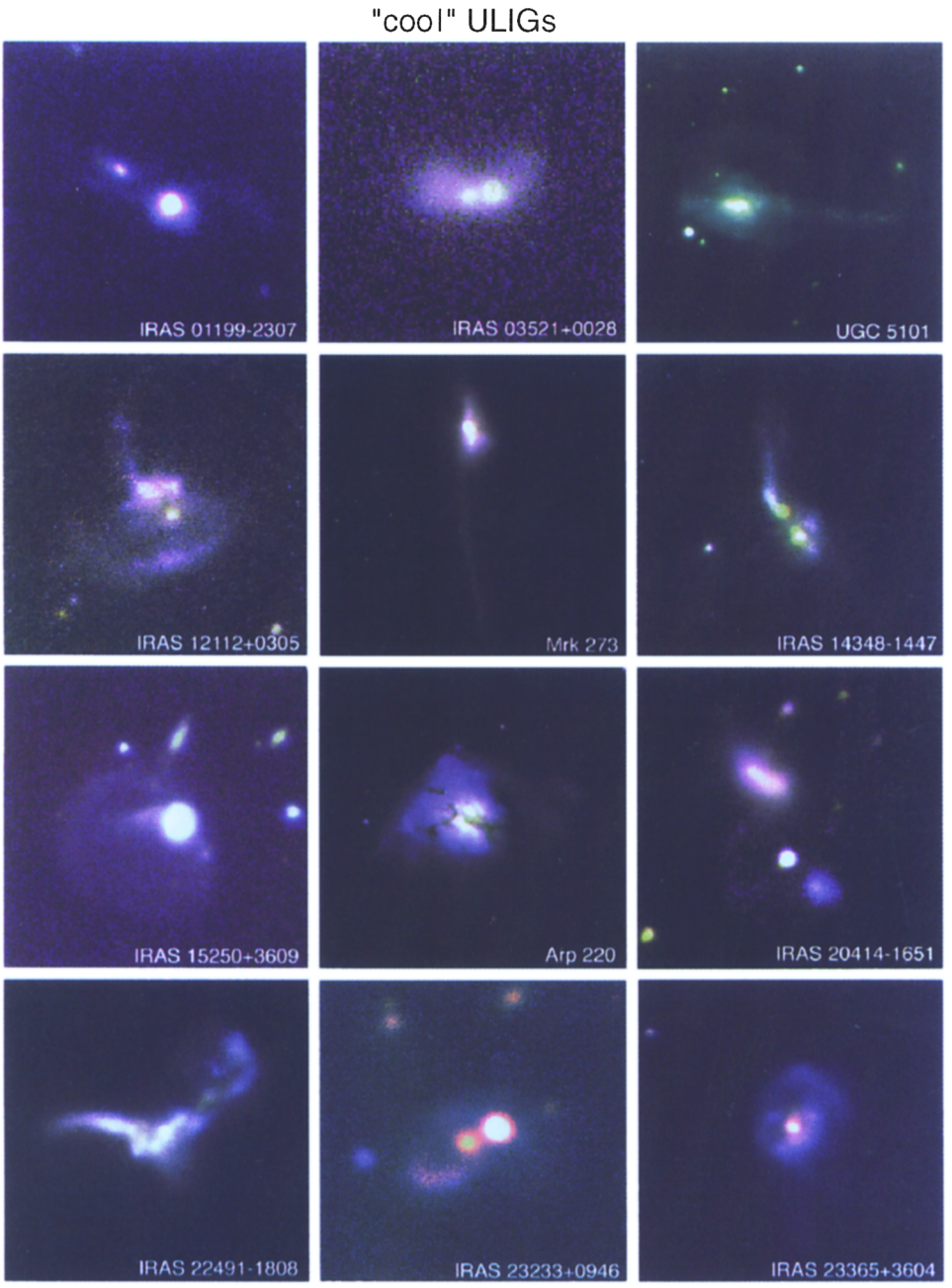

Plate 7. Near truecolor images of a complete sample of "cool" ($f_{25}/f_{60} < 0.2$) ULIGs constructed from B& I-band ground-based data (Surace 1998). [see Sanders et al., p. 290]

https://doi.org/10.1017/S0074180900112124 Published online by Cambridge University Press

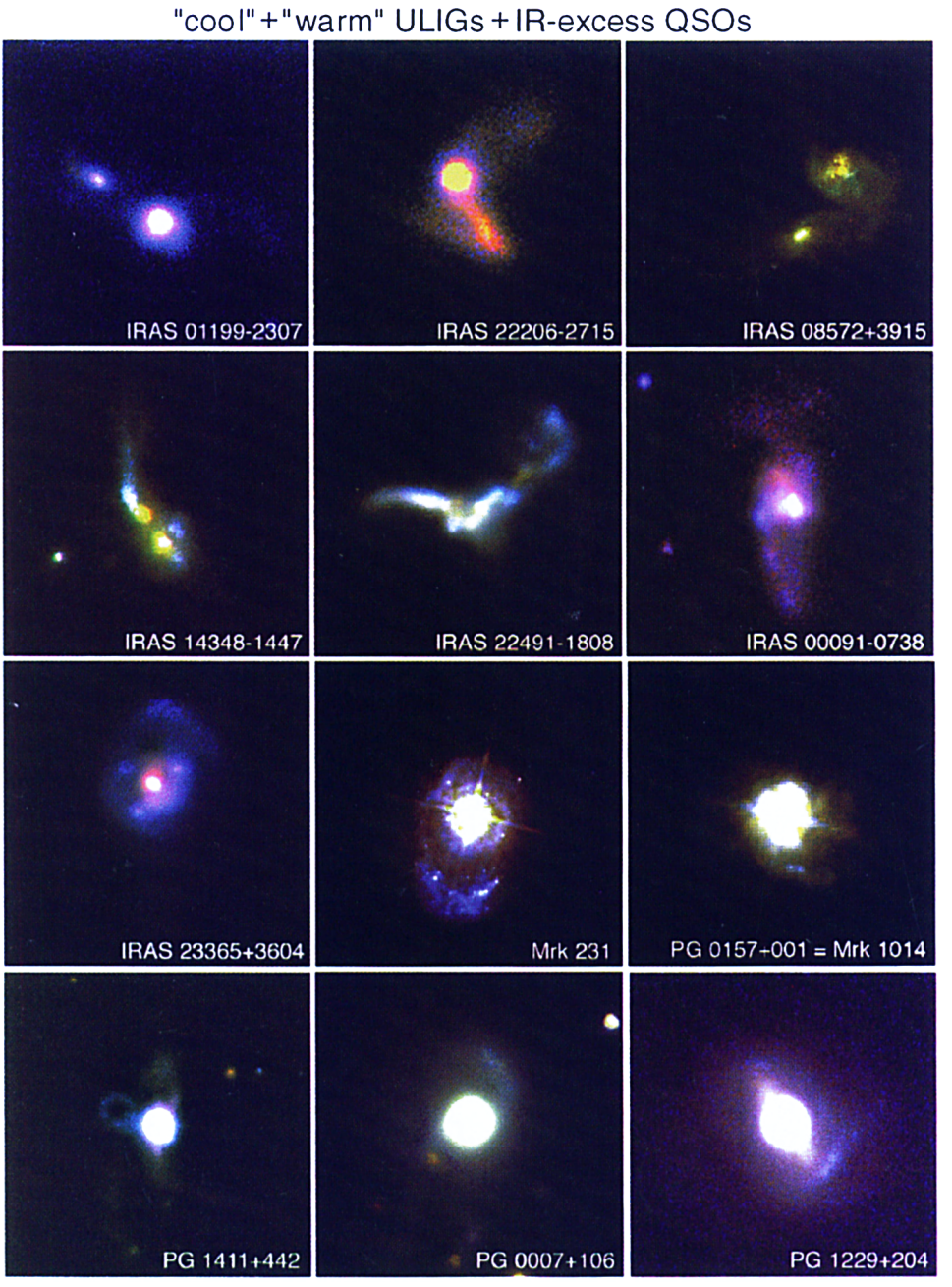

Plate 8. Near truecolor images of ULIGs arranged according to FIR color temperature, with (from upper left) "cool" ($f_{25}/f_{60} < 0.2$) ULIGs (panels 1-5), "warm" ($f_{25}/f_{60} > 0.2$) ULIGs (panels 6-8), and IR-excess ($L_{\rm ir}/L_{\rm B} > 1$) PGQSOs (panels 9-12). [see Sanders et al., p. 290, and Surace & Sanders, p. 363]

https://doi.org/10.1017/S0074180900112124 Published online by Cambridge University Press